Temperature dependence of the magnetization of superlattices with variable interlayer magnetic couplings

Z. Q. Qiu, J. E. Mattson, C. H. Sowers, U. Welp, and S. D. Bader
Material Science Division, Argonne National Laboratory, Argonne, Illinois 60439

H. Tang and J. C. Walker
Department of Physics, The Johns Hopkins University, Baltimore, Maryland 21218
(Received 29 July 1991)

A Heisenberg model is solved for the coupling of two-dimensional ferromagnetic layers separated by nonmagnetic spacer layers in a superlattice configuration. The cases of noncoupling, and ferromagnetic and anti-ferromagnetic interlayer couplings, are solved for the temperature dependence of the magnetization at low temperature; the results yield linear, $T^{3/2}$ and T^2 power laws, respectively. Experimental realization of the coupling cases was then sought. Three sputtered Fe/Cr superlattices with 10 Å Fe layers and Cr-layer thicknesses of 100, 20, and 10 Å were chosen to span the three cases, respectively. Superconducting-quantum-interference-device magnetometry yields linear and $T^{3/2}$ behavior for the first two cases. Mössbauer spectroscopy in zero field indicates an approximately T^2 behavior for the antiferromagnetically coupled sample. The results are discussed and related to recent magnetotransport work.

I. INTRODUCTION

Recently great effort has been devoted to investigate the magnetic coupling of ferromagnetic films across nonmagnetic spacer layers. In particular, the discovery of antiferromagnetic (AF) coupling in Fe/Cr/Fe sandwich structures[1] and the associated giant magnetoresistance in Fe/Cr superlattices[2] has stimulated both experimental[3] and theoretical[4] interest in the search for new materials and the quest to unravel the underlying mechanisms.[5] A number of systems, such as Co/Ru,[3] Fe/Cu,[6] Fe/Mo,[7] Co/Cu,[8] Ni/Ag,[9] etc., have been found to exhibit similar behavior to the Fe/Cr system, and it is accepted that the interlayer coupling plays a crucial role in determining the magnetic and electronic-transport properties of this newly emerging class of materials.[4] In order to understand better the effect of the interlayer coupling on the magnetic properties, we present an investigation of the temperature dependence of the magnetization $M(T)$ in magnetic-nonmagnetic superlattices. A specific motivation to examine $M(T)$ for Fe/Cr superlattices is that in a recent experimental study of the T dependence of the resistivity of this system by Mattson *et al.*,[10] a T^2 behavior was found for the drop in magnetoresistance from its low-T limiting value, and was attributed to the thermal population of magnons. The question is whether the gross magnon spectrum, as monitored by $M(T)$, behaves similarly to the interfacial magnons that presumably dominate the T dependence of the transport properties.

Although the magnetization of thin films[11,12] and at the surface of semi-infinite solids[13] has been treated theoretically rather extensively over the years, the magnetization of coupled layers is a relatively unexplored field until recently. Qiu and Walker[14] used a Heisenberg model to treat the case of ferromagnetic layers coupled ferromagnetically, and found that the $T^{3/2}$ Bloch law persists at low T with a weakened spin-wave stiffness constant. Similar conclusions pertain to the surface of semi-infinite ferromagnets.[12] Also, Singh *et al.*[15] used a Hubbard model to derive spin-wave expressions for AF layers that are weakly coupled together antiferromagnetically, and found a T^2 behavior at low T that can cross over to a two-dimensional (2D) $[T \ln T]$ expression on warming as the thermal energy exceeds the interlayer-coupling strength. They compared their results to experimental $M(T)$ data for AF oxide insulators that can be doped to become high-temperature superconductors.

In the present work we construct a Heisenberg model to calculate $M(T)$ for ferromagnetic-nonmagnetic superlattices, and treat both ferromagnetic and AF interlayer-coupling cases in Sec. II. We then present superconducting-quantum-interference-device (SQUID) magnetometry and Mössbauer measurements for Fe/Cr superlattices and compare experiment to our theoretical results in Sec. III. We discuss the relationship of our findings to the magnetotransport behavior in Sec. IV, and summarize our findings in Sec. V.

II. DESCRIPTION OF THE THEORETICAL CALCULATION

A. Heisenberg model

Consider a ferromagnetic-nonmagnetic superlattice with the film parallel to the xy plane. If the ferromagnetic layer is thin enough to behave like a 2D system, we can approximately model each individual ferromagnetic layer by a 2D square lattice of lattice constant a. Then we can map the ferromagnetic component of the superlattice onto a 3D cubic lattice in which each plane parallel to the xy plane corresponds to a ferromagnetic layer in the superlattice. The lattice constant b along the z axis,

then, corresponds to the spacing between two adjacent ferromagnetic layers. In this work, we will only consider Heisenberg-type nearest-neighbor interactions. Suppose that each lattice site $\boldsymbol{l}=(l_x,l_y,l_z)$ is assigned a spin $\mathbf{S}(\boldsymbol{l})$. Then, the nearest-neighbor interaction is introduced as follows: The interaction is J_0 between nearest neighbors with the same l_Z value, and it is $+J_1$ (or $-J_1$) between nearest neighbors with different l_Z values. In this way, J_0 is the ferromagnetic exchange interaction of the ferromagnetic film, and J_1 (or $-J_1$) is the ferromagnetic (or AF) interlayer coupling between the ferromagnetic films. From the above description, we see that our model is only valid for a superlattice with the ferromagnetic film thin enough to behave two-dimensionally. In the following, we will apply spin-wave theory to calculate $M(T)$ for both AF and ferromagnetic interlayer-coupling cases.

B. Antiferromagnetic coupling case

In this case, the Hamiltonian of the system is

$$H=-J_0\sum_{l_z}\sum_{\boldsymbol{l}_\parallel,\delta}\mathbf{S}(\boldsymbol{l}_\parallel,l_z)\cdot\mathbf{S}(\boldsymbol{l}_\parallel+\boldsymbol{\delta},l_z)+J_1\sum_{l_z,\boldsymbol{l}_\parallel}[\mathbf{S}(l_z,\boldsymbol{l}_\parallel)\cdot\mathbf{S}(l_z-1,\boldsymbol{l}_\parallel)+\mathbf{S}(l_z,\boldsymbol{l}_\parallel)\cdot\mathbf{S}(l_z+1,\boldsymbol{l}_\parallel)] .$$

Here $\boldsymbol{l}_\parallel=(l_x,l_y,0)$, and $\boldsymbol{\delta}$ is the nearest-neighbor vector in the xy plane. The first term in the Hamiltonian represents a simple sum within the 2D layers, while the second term represents the interlayer coupling between adjacent layers. In this paper, we will assume that the easy magnetization axis is perpendicular to the plane of the film, i.e., along the z axis. This assumption is not crucial, however, and our results can be easily extended to the in-plane easy-axis case. At $T=0$ K, all spins on each ferromagnetic sheet are aligned in the same direction (either along $+\hat{\mathbf{z}}$ or $-\hat{\mathbf{z}}$), while the spins on adjacent ferromagnetic sheets are aligned oppositely due to the AF interlayer coupling. Thus, we can divide the lattice into two sublattices: $(l_x,l_y,l_z=nb)\in A$, if n is an odd integer; and $(l_x,l_y,l_z=nb)\in B$, if n is even; where all spins on sublattice A are along $+\hat{\mathbf{z}}$ and all spins on sublattice B are along $-\hat{\mathbf{z}}$. For $k_BT\ll J_0$, the change of the z component of the spin ΔS_z due to the thermal excitations is much smaller than S itself, so that we can apply the Holstein-Primakoff transformation[16] within each sublattice A and B. The resulting Hamiltonian in k space is

$$H=\sum_{\mathbf{k}}[\omega_0(\mathbf{k}_\parallel)+4SJ_1][a^\dagger(\mathbf{k})a(\mathbf{k})+b^\dagger(\mathbf{k})b(\mathbf{k})]+4SJ_1\sum_{\mathbf{k}}\cos(k_zb)[a(\mathbf{k})b(\mathbf{k})+a^\dagger(\mathbf{k})b^\dagger(\mathbf{k})]+\text{c.c.}$$

and

$$S_z(\boldsymbol{l})=S-\frac{a^2b}{(2\pi)^3}\int d^3k\,\langle a^\dagger(\mathbf{k})a(\mathbf{k})\rangle_T \quad \text{for } \boldsymbol{l}\in A ,$$

and

$$S_z(\boldsymbol{l})=-S+\frac{a^2b}{(2\pi)^3}\int d^3\langle b^\dagger(\mathbf{k})b(\mathbf{k})\rangle_T \quad \text{for } \boldsymbol{l}\in B .$$

Here $\langle\cdots\rangle_T$ stands for the thermal average, and $\omega_0(\mathbf{k}_\parallel)$ is the 2D ferromagnetic spin-wave energy:

$$\omega_0(\mathbf{k}_\parallel)=4SJ_0[2-\cos(k_xa)-\cos(k_ya)] .$$

The $a(\mathbf{k}),a^\dagger(\mathbf{k})$ and $b(\mathbf{k})b^\dagger(\mathbf{k})$ pairs are the $\mathbf{k}$-dependent magnon annihilation and creation operators within the A and B sublattices. They satisfy the boson commutation relations:

$$[a(\mathbf{k}),a^\dagger(\mathbf{k}')]=[b(\mathbf{k}),b^\dagger(\mathbf{k}')]=\delta(\mathbf{k},\mathbf{k}') ,$$
$$[a(\mathbf{k}),b(\mathbf{k}')]=[a(\mathbf{k}),b^\dagger(\mathbf{k}')]=0 .$$

If we define

$$\omega(\mathbf{k})=\sqrt{[\omega_0(\mathbf{k})+4SJ_1]^2-[4SJ_1\cos(k_zb)]^2} ,$$

it is easy to show that the following transformation:

$$\alpha(\mathbf{k})=a(\mathbf{k})\left[\frac{\omega_0(\mathbf{k}_\parallel)+4SJ_1}{2\omega(\mathbf{k})}+\frac{1}{2}\right]^{1/2}+b^\dagger(\mathbf{k})\left[\frac{\omega_0(\mathbf{k}_\parallel)+4SJ_1}{2\omega(\mathbf{k})}-\frac{1}{2}\right]^{1/2} ,$$
$$\beta(\mathbf{k})=a^\dagger(\mathbf{k})\left[\frac{\omega_0(\mathbf{k}_\parallel)+4SJ_1}{2\omega(\mathbf{k})}-\frac{1}{2}\right]^{1/2}+b(\mathbf{k})\left[\frac{\omega_0(\mathbf{k}_\parallel)+4SJ_1}{2\omega(\mathbf{k})}+\frac{1}{2}\right]^{1/2}$$

also satisfies the boson commutation relations:

$$[\alpha(\mathbf{k}),\alpha^\dagger(\mathbf{k}')]=[\beta(\mathbf{k}),\beta^\dagger(\mathbf{k}')]=\delta(\mathbf{k},\mathbf{k}') ,$$
$$[\alpha(\mathbf{k}),\beta(\mathbf{k}')]=[\alpha(\mathbf{k}),\beta^\dagger(k')]=0$$

and diagonalizes the Hamiltonian, such that

$$H=\sum_{\mathbf{k}}\omega(\mathbf{k})[\alpha^\dagger(\mathbf{k})\alpha(\mathbf{k})+\beta^\dagger(\mathbf{k})\beta(\mathbf{k})]+E_0 .$$

Thus, E_0 is the zero-point energy and $\omega(\mathbf{k})$ is the spin-wave energy of the system. Therefore, we can obtain the thermal average of the following products:

$$\langle\alpha^\dagger(\mathbf{k})\alpha(\mathbf{k})\rangle_T=\langle\beta^\dagger(\mathbf{k})\beta(\mathbf{k})\rangle_T=\frac{1}{e^{\omega(\mathbf{k})/k_BT}-1} ,$$

$$\langle\alpha(\mathbf{k})\alpha(\mathbf{k})\rangle_T=\langle\beta(\mathbf{k})\beta(\mathbf{k})\rangle_T=\langle\alpha(\mathbf{k})\beta(\mathbf{k})\rangle_T=\langle\alpha(\mathbf{k})\beta^\dagger(\mathbf{k})\rangle_T=0 .$$

Then by transforming $\alpha(\mathbf{k}),\beta(\mathbf{k})$ into $a(\mathbf{k}),b(\mathbf{k})$, we get

$$\langle a^\dagger(\mathbf{k})a(\mathbf{k})\rangle_T=\langle b^\dagger(\mathbf{k})b(\mathbf{k})\rangle_T=\frac{\omega_0(\mathbf{k}_\parallel)+4SJ_1}{\omega(\mathbf{k})}\frac{1}{e^{\omega(\mathbf{k})/k_BT}-1}+\left[\frac{\omega_0(\mathbf{k}_\parallel)+4SJ_1}{2\omega(\mathbf{k})}-\frac{1}{2}\right] ,$$

where the last term is T independent and represents the zero-point quantum spin fluctuation. In the present work, we are only interested in the T-dependent part, so we can drop the second term and obtain

$$\Delta S_z(T) \equiv S - |S_z(l)| = \frac{a^2 b}{(2\pi)^3} \int d^3k \frac{\omega_0(\mathbf{k}_\parallel) + 4SJ_1}{\omega(\mathbf{k})} \frac{1}{e^{\omega(\mathbf{k})/k_B T} - 1} .$$

For $k_B T \ll J_0$, only spin waves with $k_x a \ll 1$ and $k_y a \ll 1$ can be excited, so that

$$\omega_0(\mathbf{k}_\parallel) \approx 2SJ_0[(k_x a)^2 + (k_y a)^2] = 2SJ_0 k_\parallel^2 a^2 ,$$

and

$$\Delta S_z(T) \approx \frac{k_B T}{16SJ_0\pi^2} \int_{-\pi}^{\pi} d(k_z b) \ln(1 - e^{-4SJ_1 |\sin(k_z b)|/k_B T}) = -\frac{k_B T}{8SJ_0\pi^2} \int_0^{\pi} d\zeta \ln(1 - e^{-4SJ_1 \sin\zeta/k_B T}) .$$

In the strong ($J_1 \gg k_B T$) and weak ($J_1 \ll k_B T$) coupling limits, we get the following T dependence:

$$\Delta S_z(T) \approx \frac{k_B T}{8SJ_0\pi^2} \int_0^{\infty} d\zeta \sum_{n=1}^{\infty} \frac{1}{n} e^{-4nSJ_1 \zeta/k_B T} = \frac{1}{3} \left[\frac{k_B T}{8SJ_0}\right] \left[\frac{k_B T}{8SJ_1}\right], \quad J_1 \gg k_B T$$

$$\Delta S_z(T) \approx -\frac{k_B T}{8SJ_0\pi^2} \int_0^{\pi} d\zeta \ln(4SJ_1 \sin\zeta/k_B T) = \frac{k_B T}{8S\pi J_0} \ln\left[\frac{k_B T}{2SJ_1}\right], \quad J_1 \ll k_B T .$$

Thus, a T^2 dependence of the sublattice magnetization is expected at low T ($J_1 \gg k_B T$), and a quasi-T linear dependence is expected at high T ($J_1 \ll k_B T$). As $J_1 \to 0$, all the ferromagnetic sheets are decoupled; so the divergence of the integral reflects the Mermin-Wagner theorem that there is no finite-temperature ordering in an isotropic 2D Heisenberg lattice.[17] We do not include magnetic anisotropy in our calculation. As has been shown previously, surface anisotropy permits the ferromagnetic 2D Heisenberg lattice to have a finite Curie temperature,[18] and introduces an energy gap in the spin-wave spectrum. The gap permits the integral of $\Delta S_z(T)$ to converge, and yields a quasilinear T dependence for the magnetization.[12]

C. Ferromagnetic coupling case

In this case, our model is an anisotropic 3D ferromagnetic lattice. The Hamiltonian of the superlattice is

$$H = -J_0 \sum_{l_z} \sum_{l_\parallel, \delta} \mathbf{S}(l_\parallel, l_z) \cdot \mathbf{S}(l_\parallel + \delta, l_z) - J_1 \sum_{l_z, l_\parallel} [\mathbf{S}(l_z, l_\parallel) \cdot \mathbf{S}(l_z - 1, l_\parallel) + \mathbf{S}(l_z, l_\parallel) \cdot \mathbf{S}(l_z + 1, l_\parallel)] .$$

At $T = 0$ K, all spins are aligned in the same direction, so it is not necessary to divide the lattice into sublattices. In this case it is easy to show that for $k_B T \ll J_0$, the Holstein-Primakoff transformation in $\mathbf{k}$ space will directly diagonolize the Hamiltonian and yield the following spin-wave spectrum:

$$\omega(\mathbf{k}) = 4SJ_0[2 - \cos(k_x a) - \cos(k_y a)] + 4SJ_1[1 - \cos(k_z b)] .$$

For $k_B T \ll J_0$, only spin waves with $k_x a \ll 1$ and $k_y a \ll 1$ can be excited so that

$$\omega(\mathbf{k}) = 2SJ_0 k_\parallel^2 a^2 + 4SJ_1[1 - \cos(k_z b)]$$

and

$$\Delta S_z(T) \approx -\frac{k_B T}{16SJ_0\pi^2} \int_{-\pi}^{\pi} d(k_z b) \times \ln(1 - e^{-4SJ_1[1 - \cos(k_z b)]/k_B T}) = -\frac{k_B T}{3SJ_0\pi^2} \int_0^{\pi} d\zeta \ln(1 - e^{-8SJ_1 \sin^2(\zeta/2)/k_B T}) .$$

In the strong ($J_1 \gg k_B T$) and weak ($J_1 \ll k_B T$) coupling limits, we get the following T dependences

$$\Delta S_z(T) \approx \frac{k_B T}{8SJ_0\pi^2} \int_0^{\infty} d\zeta \sum_{n=1}^{\infty} \frac{1}{n} e^{-2nSJ_1 \zeta^2/k_B T} = \left[\frac{k_B T}{8S\pi J_0}\right] \left[\frac{k_B T}{8S\pi J_1}\right]^{1/2} \sum_{n=1}^{\infty} \frac{1}{n^{3/2}}, \quad J_1 \gg k_B T$$

$$\Delta S_z(T) \approx = -\frac{k_B T}{8SJ_0\pi^2} \int_0^{\pi} d\zeta \ln[8SJ_1 \sin^2(\zeta/2)/k_B T] = \frac{k_B T}{8S\pi J_0} \ln\left[\frac{k_B T}{2SJ_1}\right], \quad J_1 \ll k_B T .$$

In the low-T region ($J_1 \gg k_B T$), we get a $T^{3/2}$ Bloch law behavior, as expected, since the system is just a 3D ferromagnetic lattice. In the high-T region ($J_1 \ll k_B T$), all ferromagnetic layers are decoupled, so we again get the quasilinear T dependence.

III. EXPERIMENTAL RESULTS

A. Sample preparation

The Fe/Cr superlattice were grown on NaCl substrates in a Microscience Researcher 101 growth chamber using dc magnetron sputtering from two Ion Tech diode guns. The base pressure of the chamber was 2×10^{-8} Torr and the argon pressure during the sputtering was 3 mTorr. The deposition rates for Fe and Cr were 1.0 Å/s and 1.8 Å/s, respectively. The use of NaCl as substrate enables the complete removal of the film from the substrate for magnetic measurement purposes. Three superlattices were fabricated with the Fe thickness fixed at 10 Å and the Cr thickness set at 10, 20, and 100 Å. The total number of bilayers in each superlattice is denoted in the subscript of the following formulas for the three samples:

$[Fe(10\ Å)/Cr(10\ Å)]_{100}$, $[Fe(10\ Å)/Cr(20\ Å)]_{50}$, and $[Fe(10\ Å)/Cr(100\ Å)]_{25}$.

Low-angle x-ray diffraction was performed to characterize the layering of the superlattice structure. The diffraction peaks are due to the constructive interference from the bilayer periodicity within the superlattice. Only two diffraction peaks were observed. The absence of high-order diffraction peaks indicates that the Fe/Cr interface is relatively rougher than that of some other systems, such as Fe/Mo in which up to seventh-order peaks were observed in the low-angle x-ray-diffraction data.[7] Nevertheless, the presence of the first- and second-order diffraction peaks reveals that we do get a layered structure of a similar quality as in our Fe/Cr superlattices grown on sapphire that were used in magnetoresisitivity studies.[10]

B. Magnetic properties

From previous work,[10] the 10-, 20-, and 100-Å thicknesses of Cr should produce the AF-coupling (AFC), ferromagnetic-coupling (FC), and noncoupling (NC) cases, respectively, between the Fe layers separated by the Cr spacer layers. For convenience we will denote the three superlattices by AFC, FC, and NC, respectively.

The magnetization measurements were taken using a Quantum Designs rf SQUID magnetometer. The samples were prepared by peeling off the film from the NaCl substrate in water and cutting the films into $\sim 3\times 4$-mm shapes. Hysteresis loops for the three films were measured at 200 K by applying the magnetic field parallel to the film plane. The results are plotted in Fig. 1. The low saturation field and the rectangular-type shape of the hysteresis loops for the FC and NC samples indicate that the easy magnetization axes are in plane. Since the thickness of Fe in the AFC sample is the same as that of the FC and NC samples, the easy axes of the AFC sample should also be in plane. The high saturation field and low remnant magnetization of the AFC sample, compared with the FC and NFC samples, demonstrate that the sample is indeed AF. From the hysteresis loop of the other two samples, we are unable to distinguish between ferromagnetic coupling and noncoupling. But, as shown in the following, measurements on $M(T)$ will clearly distinguish between the two cases.

$M(T)$ of the FC and NC samples was measured by saturating the specimen at 4 kG. This magnetic field will open an energy gap in the spin-wave spectrum of magnitude of only $\sim\mu H\approx 8\times 10^{-17}$ erg, which is equivalent to a thermal energy of ≈ 0.6 K. Thus, the application of the magnetic field has negligible effect on $M(T)$ in the T range studied. The $M(T)$ results for the FC and NC samples are plotted in Fig. 2. It can be seen that the NC sample shows a linear T dependence of M, while the FC sample shows a $T^{3/2}$ dependence. The solid lines in Fig. 3 are fitted to T^n power laws with $n=0.98$ and $n=1.50$ correspondingly. In order to see the power law more clearly, double-logarithmic $[\Delta M/M(0)] \equiv [1-M(T)/M(0)]$ vs T plots for the two samples are shown in Fig. 3. The straight lines in the log-log plots

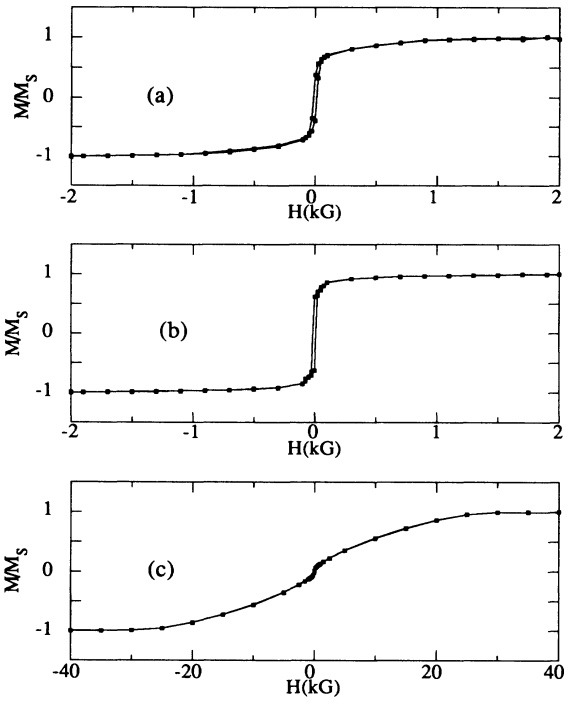

FIG. 1. Hysteresis loops of the (a) noncoupling (NC), (b) ferromagnetic-coupling (FC), and (c) antiferromagnetic-coupling (AFC) samples.

demonstrate the power-law behavior of $M(T)$, and the slopes give the values of the exponents of $0.98\approx 1.0$ and $1.50=\frac{3}{2}$, as anticipated from the theoretical derivations in Sec. II. The parameters of the fittings are listed in Table I. The T and $T^{3/2}$ dependences of the experimental results indicate that our theoretical model is quite appropriate for the ferromagnetic coupling and noncoupling cases.

The verification of the T^2 dependence for the AF coupling case requires zero-field measurements. Unfortunately, the SQUID technique is not capable of that.

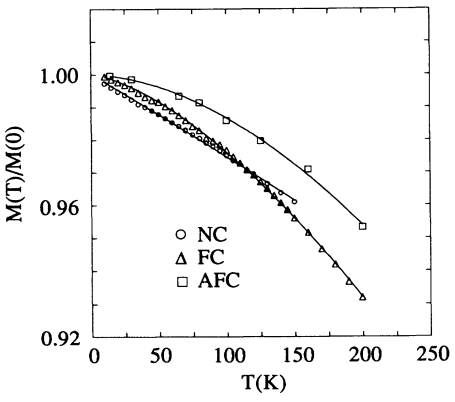

FIG. 2. Temperature dependence of the magnetization of the NC, FC, and AFC samples, which show T, $T^{3/2}$ and T^2 power laws, correspondingly. The NC and FC samples were measured by SQUID magnetometer and the AFC sample was measured by Mössbauer spectroscopy.

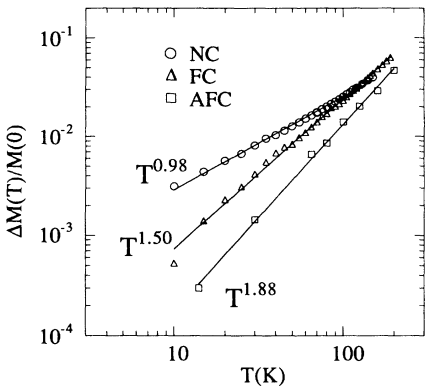

FIG. 3. Log-Log plot of $\Delta M(T)$ vs T. The straight lines show the power-law behaviors and the slopes give the temperature exponents.

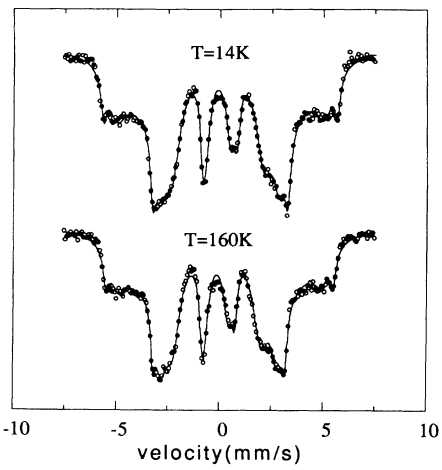

FIG. 4. The Mössbauer spectra of the AF sample at 14 and 160 K. The solid lines are results of the three-component fitting procedure summarized in Table II.

Application of a small field should maintain the AF structure and provide a nonzero magnetic component $M\cos\theta$ that represents the projection of the two canted sublattices onto the direction of the applied field, but we found that the temperature dependence of $M\cos\theta$ depends on the magnetization history and is not a well-understood quantity. Instead, we employed transmission Mössbauer spectroscopy, which offers a zero-field alternative measurement technique. It is generally acknowledged that the Mössbauer hyperfine field has the same T dependence as the magnetization. In fact, the Mössbauer technique has been used quite frequently to study $M(T)$ of ferromagnetic thin films.[19–21]

Typical Mössbauer spectra for the AF sample are shown in Fig. 4. First, notice that the intensity ratio of the inner, middle, and outer peaks is roughly 1:4:3, indicating that the magnetization of the film is perpendicular to the incident γ-ray direction. Since the film is also perpendicular to the incident γ-ray direction, the intensity ratio indicates that the magnetization is in plane, which is consistent with the SQUID magnetometry results. Second, the relatively broad linewidth implies a multicomponent spectrum. We use three components to fit the spectrum. The results are depicted by the solid lines in Fig. 4 and the fitted parameters for the 14-K spectrum are listed in Table II. The hyperfine-field data for the first component has the smallest error of the three components, so we use it to study the temperature dependence. The result is plotted in Figs. 2 and 3. The fitted parameters are listed in Table I. We see that $M(T)$ of the AF sample has a $T^{1.88}$ behavior, close to the T^2 law predicted by our model. By assuming that $S=\frac{1}{2}$ and that J_0 has the bulk-Fe value, we also can estimate the interlayer-coupling strength J_1 for the ferromagnetic and AF samples. These estimates are also included in Table I. The J_1 value of 1.5 meV for the AF sample agrees very well with the value of 1.38 meV of Barthélémy *et al.*[22]

TABLE I. Magnetization fitted to $M(T)/M(0)=1-bT^n$ for the three samples which correspond to the noncoupling (NC), ferromagnetic-coupling (FC), and antiferromagnetic-coupling (AFC) cases.

Sample	n	b (K^{-n})	J_1 (meV)
NC	0.98±0.01	$(2.8\pm0.1)\times10^{-4}$	
FC	1.50±0.02	$(2.4\pm0.2)\times10^{-5}$	1.8±0.2
AFC	1.88±0.02	$(2.3\pm0.2)\times10^{-6}$	1.5±0.1

IV. DISCUSSION

The experimental data for the ferromagnetic and noncoupled cases agree with expectations, based on the derivations presented herein, and with previous work for ferromagnetic films and 2D films.[21,23] The question of interest is to examine the limitations of our approach as it is applied to the AF case. The theoretical derivation applied strictly for coupled Fe monolayers, while the measured film actually had 10-Å-thick Fe layers. Therefore, the spin-wave excitations along the normal direction of the film are not only due to the interlayer AF coupling, but also to the ferromagnetic exchange interaction within each Fe layer. The *intralayer* ferromagnetic characteristics may effectively reduce the exponent from 2 to 1.88 in the AF film. Finally, the model does not take into account magnetic anisotropy. This might reduce the experimental T range that lies within the low-T limits. But we have no reason to believe that the predicted T^2 behavior would emerge any more clearly if we were to constrain the fitting range to a smaller or lower T interval. It

TABLE II. Mössbauer hyperfine (H_{hf}), isomer shift (IS) and quadrupole splitting (QS) of the antiferromagnetically-coupled sample at $T=14$ K.

Component	H_{hf} (kG)	IS (mm/s)	QS (mm/s)
1	351.4±0.5	0.019±0.005	−0.007±0.005
2	311.0±1.5	0.009±0.009	−0.007± 0.008
3	237.5±1.8	−0.07±0.01	0.00±0.01

would be instructive to examine films with thinner Fe layers, and to find complementary measurement techniques, such as polarized neutron diffraction, to obtain the information of interest for the AF case.

A second issue of importance concerns the relationship of the present work to our earlier resistivity study in which we found a T^2-magnetoresistivity behavior at low T for the AF samples for Fe films even thicker than 10 Å. This suggests that the magnon spectrum is weighted differently in the two experiments. The transport behavior should have enhanced sensitivity to the interfacial magnon.[24] Our results, therefore, might just be an indication that the thermal excitation of interfacial magnons occurs with a different T dependence than that of the gross magnon spectrum. This would require further theoretical study. From this vantage point, however, it is interesting to observe that our 2D model yields a T^2 dependence of the magnetization. In Ref. 10 we observed that the magnetoresistivity has a T^2 dependence which is attributed to the thermal population of magnons. Thus from the present work, we can now see the direct correlation between the spin-wave excitations and the temperature dependence of the magnetoresistivity.

V. SUMMARY

Theoretical calculations of $M(T)$ were performed for ferromagnetic-nonmagnetic superlattices for ferromagnetic layers thin enough to behave two-dimensionally. Linear, $T^{3/2}$, and T^2 dependences of the magnetization were predicted at low T for the noncoupling, ferromagnetic-coupling, and AF-coupling cases, respectively. Sputtered Fe/Cr superlattices with component thicknesses corresponding to these three cases were fabricated and measured by means of SQUID magnetometry. The linear and $T^{3/2}$ power laws were verified for the noncoupling and ferromagnetic-coupling samples, respectively. The AF sample was measured in zero applied field by Mössbauer spectroscopy which yielded a $T^{1.88}$ dependence, close to the T^2 law predicted from our model.

ACKNOWLEDGMENTS

This work was supported by the U.S. Department of Energy, BES-Materials Sciences under Contract No. W-31-109-ENG-38. J.E.M. was supported by NSF-MRG Contract No. DMR-86-03304.

[1]P. Grünberg, R. Schreiber, Y. Pang, M. B. Brodsky, and C. H. Sowers, Phys. Rev. Lett. **57**, 2442 (1986).

[2]M. N. Baibich, J. M. Broto, A. Fert, F. Nguyen Van Dau, F. Petroff, P. Etienne, G. Greuzet, A. Friedrich, and J. Chazelas, Phys. Rev. Lett. **61**, 2472 (1988).

[3]S. S. P. Parkin, N. More, and K. P. Roche, Phys. Rev. Lett. **64**, 2304 (1990).

[4]P. M. Levy, S. Zhang, and A. Fert, Phys. Rev. Lett. **65**, 1643 (1990); Y. Wang, P. M. Levy, and J. L. Fry, *ibid.* **65**, 2732 (1990).

[5]J. Ungaris, R. J. Celotta, and D. T. Pierce, Phys. Rev. Lett. **67**, 140 (1991).

[6]B. Heinrich, Z. Celinski, J. F. Cochran, W. B. Muir, J. Rudd, Q. M. Zhong, A. S. Arrott, K. Myrtle, and J. Kirschner, Phys. Rev. Lett. **64**, 673 (1990); W. R. Bennett, W. Schwarzacher, and W. F. Egelhoff, Jr., *ibid.* **65**, 3169 (1990).

[7]M. E. Brubaker, J. E. Mattson, C. H. Sowers, and S. D. Bader, Appl. Phys. Lett. **58**, 2306 (1991).

[8]S. S. P. Parkin, R. Bhadra, and K. P. Roche, Phys. Rev. Lett. **66**, 2152 (1991); S. S. P. Parkin, Z. G. Li, and D. J. Smith, Appl. Phys. Lett. **58**, 2710 (1991).

[9]C. A. dos Santos, B. Rodmacq, M. Vaezzadeh, and B. George, Appl. Phys. Lett. **59**, 126 (1991).

[10]J. E. Mattson, M. E. Brubaker, C. H. Sowers, M. Conover, Z. Qiu, and S. D. Bader, Phys. Rev. B **44**, 9378 (1991).

[11]J. C. Levy and J. L. Motchane, J. Vac. Sci. Technol. **9**, 721 (1971).

[12]R. Navarro and L. J. Dejongh, Physica B+C **98B**, 1 (1979).

[13]S. J. Glass and M. J. Klein, Phys. Rev. **109**, 288 (1958); D. L. Mills and A. A. Maradudin, J. Phys. Chem. Solids **28**, 1855 (1967); J. Mathon and S. B. Ahmad, Phys. Rev. B **37**, 660 (1988); G. T. Rado, *ibid.* **40**, 407 (1989).

[14]Z. Q. Qiu and J. C. Walker, J. Appl. Phys. **67**, 5643 (1990).

[15]A. Singh, Z. Tešanović, H. Tang, G. Xiao, C. L. Chien, and J. C. Walker, Phys. Rev. Lett. **64**, 2571 (1990).

[16]T. Holstein and H. Primakoff, Phys. Rev. **58**, 1098 (1940).

[17]M. D. Mermin and H. Wagner, Phys. Rev. Lett. **17**, 1133 (1966).

[18]M. Bander and D. L. Mills, Phys. Rev. B **38**, 12 015 (1988).

[19]J. C. Walker, R. Droste, G. Stern, and J. Tyson, J. Phys. (Paris) Colloq. **45**, C5-357 (1984).

[20]M. Przybylski and U. Gradmann, Phys. Rev. Lett. **59**, 1152 (1987).

[21]G. Bayreuther and G. Lugert, J. Magn. Magn. Mater. **35**, 50 (1983).

[22]A. Barthélémy, A. Fert, M. N. Baibich, S. Hadjoudj, and F. Petroff, J. Appl. Phys. **67**, 5908 (1990).

[23]D. Mauri, D. Scholl, H. C. Siegmann, and E. Kay, Phys. Rev. Lett. **62**, 1900 (1989).

[24]S. Zhang and P. M. Levy, Phys. Rev. B **43**, 11 048 (1991).